Cell Reports

Peak BMP Responses in the *Drosophila* Embryo Are Dependent on the Activation of Integrin Signaling

Graphical Abstract

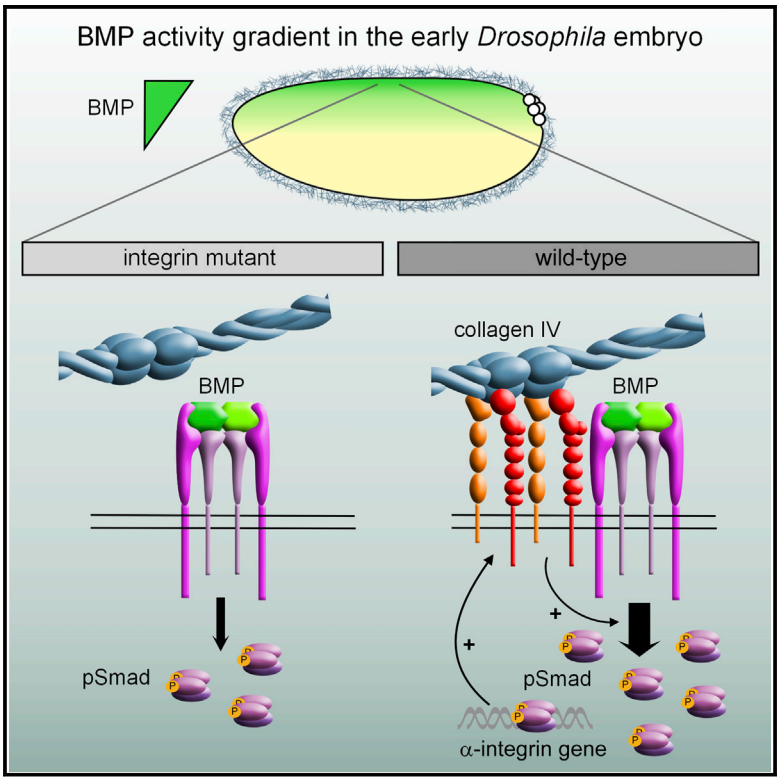

Highlights

- *Drosophila* embryos lacking integrin function have disrupted BMP responses
- Collagen IV activates integrin signaling to enhance levels of the pMad transducer
- Integrins bind BMP receptors and promote pMad levels after BMP receptor activation
- BMP activates expression of an α-integrin, representing a positive feedback loop

Authors

Annick Sawala, Margherita Scarcia, Catherine Sutcliffe, Scott G. Wilcockson, Hilary L. Ashe

Correspondence

hilary.ashe@manchester.ac.uk

In Brief

During development, cells receive information from the extracellular matrix via integrin receptors, in addition to growth factor signals from other cells. Sawala et al. show that BMP-responsive transcription in the *Drosophila* embryo is not simply a readout of the BMP concentration but also requires integrin-mediated enhancement of BMP signal transduction.

Sawala et al., 2015, Cell Reports *12*, 1584–1593
September 8, 2015
http://dx.doi.org/10.1016/j.celrep.2015.08.012

OPEN ACCESS
CellPress

Cell Reports
Report

Peak BMP Responses in the *Drosophila* Embryo Are Dependent on the Activation of Integrin Signaling

Annick Sawala,[1,2] Margherita Scarcia,[1] Catherine Sutcliffe,[1] Scott G. Wilcockson,[1] and Hilary L. Ashe[1,*]
[1]Faculty of Life Sciences, University of Manchester, Manchester M13 9PT, UK
[2]Present address: The Francis Crick Institute, Mill Hill Laboratory, The Ridgeway, London NW7 1AA, UK
*Correspondence: hilary.ashe@manchester.ac.uk
http://dx.doi.org/10.1016/j.celrep.2015.08.012

SUMMARY

Within a 3D tissue, cells need to integrate signals from growth factors, such as BMPs, and the extracellular matrix (ECM) to coordinate growth and differentiation. Here, we use the *Drosophila* embryo as a model to investigate how BMP responses are influenced by a cell's local ECM environment. We show that integrins, which are ECM receptors, are absolutely required for peak BMP signaling. This stimulatory effect of integrins requires their intracellular signaling function, which is activated by the ECM protein collagen IV. Mechanistically, integrins interact with the BMP receptor and stimulate phosphorylation of the downstream Mad transcription factor. The BMP-pathway-enhancing function of integrins is independent of focal adhesion kinase, but it requires conserved NPXY motifs in the β-integrin cytoplasmic tail. Furthermore, we show that an α-integrin subunit is a BMP target gene, identifying positive feedback between integrin signaling and BMP pathway activity that may contribute to robust cell fate decisions.

INTRODUCTION

Two key requirements for the success of multicellular life are the ability of cells to adhere to each other, via a secreted protein network called the extracellular matrix (ECM), and to communicate with each other, sometimes over long distances, through the release of signaling molecules. In addition to providing structural support to tissues, the ECM has evolved to regulate intercellular signaling pathways, for example by binding to growth factors and regulating their distribution or activity in the extracellular space (Hynes, 2009). The ECM can also signal through its own adhesion receptors, primarily integrins, to initiate intracellular signaling events that converge with growth factor signaling pathways, thus allowing cells to integrate information about ECM composition and mechanical properties with biochemical signals (Giancotti and Ruoslahti, 1999).

Although crosstalk between integrin signaling and growth-factor-activated receptor tyrosine kinase signaling has been studied in some detail (Alam et al., 2007), comparably little is known about how the ECM influences intracellular signaling through bone morphogenetic proteins (BMPs), a highly conserved family of growth factors with diverse roles during development and disease (Wu and Hill, 2009). In the canonical signaling pathway, BMPs assemble complexes of type I and type II receptors, leading to activation of the type I receptor Ser/Thr kinase domain and phosphorylation of a Smad transcription factor (Mad in *Drosophila*) (Wu and Hill, 2009). Phospho-Mad (pMad) associates with a second Smad transcription factor (Medea in *Drosophila*), and the pMad/Medea complex accumulates in the nucleus to regulate transcription of BMP target genes. Using the *Drosophila* model, we have recently shown that the ECM molecule collagen IV directly binds BMPs and regulates their movement across tissues (Sawala et al., 2012; Wang et al., 2008). Several findings indicate that collagen IV may also act locally to enhance BMP signal reception. For example, collagen IV is required for local activation of BMP signaling at the tip of developing renal tubules (Bunt et al., 2010). Furthermore, collagen IV can enhance the effect of BMPs in tissue culture, where long-range movement is unlikely to be important (Paralkar et al., 1992).

To understand how the local ECM environment impacts BMP responses, we investigated a role for integrins, which are collagen IV receptors (Khoshnoodi et al., 2008). We find that maximal levels of BMP pathway activation in vivo are only achieved in the presence of integrin signaling, which functions downstream of collagen IV to potentiate signaling through the canonical Smad pathway.

RESULTS

Integrins Are Required for Peak Levels of BMP Signaling in the Early *Drosophila* Embryo

We examined a role for integrins in BMP pathway activation in the early *Drosophila* embryo, where a BMP activity gradient specifies cell fates along the dorsoventral axis (Figure 1A). Integrin receptors are expressed on the cell surface as α/β heterodimers (Leptin et al., 1989). As βPS is the only β-integrin expressed in the early blastoderm embryo (Figure S1A), we induced homozygous germline clones for a null allele of βPS, mys^{XG43} (Leptin et al., 1989), and analyzed BMP target gene expression in embryos lacking maternal and zygotic βPS expression and therefore all integrin function (from now on referred to as βPS^{-} embryos). In wild-type embryos, the high threshold BMP target genes *Race* (*Ance* in FlyBase) and *hindsight* (*hnt*) are expressed in a narrow stripe along the dorsal midline (presumptive

amnioserosa), where peak signaling occurs, while the lower threshold gene *u-shaped* (*ush*) is expressed in a broader dorsal domain (Figure 1B). By contrast, in βPS^{-} embryos, *Race* and *hnt* expression is lost in the presumptive amnioserosa, and *ush* expression is significantly ($p < 0.0001$) narrower (Figure 1B), characteristic of embryos with reduced levels of BMP signaling. The BMP defect is rescued by a paternal wild-type copy of βPS (data not shown). Expression of the major BMP ligand in the early embryo, *dpp*, and of *sog*, which encodes a critical extracellular BMP regulator (Wu and Hill, 2009), is unaffected in βPS^{-} embryos (Figure S2A). Together, these data indicate that integrins are required for normal levels of BMP signaling in the early embryo.

As βPS can form receptors with several α-integrins (Brown, 2000), we examined BMP phenotypes in α-integrin mutant embryos. Out of the five α-integrin genes, we found that *multiple edematous wings* (*mew*) and *scab* (*scb*) are expressed in partially overlapping domains in the dorsal ectoderm (Figures S1B and S1C), where BMP signaling is active. In addition, *mew* expression extends ventrally into the neuroectoderm, overlapping with the expression domain of *sog* (Figure S1D). Embryos mutant for *mew* or *scb* exhibit defects in the expression of BMP target genes (Figure 1C), with differences in the phenotypes for *mew* and *scb* mutants reflecting their different expression patterns in the embryo. For *Race*, the expression is preferentially lost in the posterior in *scb* mutant embryos, whereas it is lost uniformly along the anterior-posterior axis in *mew* mutants (compare embryos classified as "weak" in Figure 1C). These results suggest that integrin receptors involving both *mew* and *scb* gene products enhance BMP signaling in the early embryo. The posteriorly expressed target gene *hnt*, like *Race*, is partially or fully lost in the *scb* mutant but infrequently lost in *mew* mutants (Figure 1C). Also, in a subset of *mew* mutants, *Race*, *hnt*, or *ush* expression is broadened, in extreme cases resembling embryos that lack Sog (Figures 1C and S2C). This likely represents a function of *mew* in regulating Sog distribution, as previously described in the developing wing (Araujo et al., 2003), in addition to its integrin signaling function described below. This second function may lead to a slightly flatter BMP gradient in *mew* mutants, thus explaining the broader *hnt* expression observed (Figure 1C), in contrast to the loss of *Race*, a gene that is absolutely dependent on the highest BMP levels.

We next quantified the pMad gradient in βPS^{-} embryos (Umulis et al., 2010) To circumvent staining variability between samples, we only compared βPS^{-} embryos to siblings that were maternal βPS^{-} zygotic βPS^{+}, as these embryos could be processed together throughout. Maternal βPS^{-} zygotic βPS^{+} embryos show no defect in BMP target gene expression or pMad activation (Figure 1D; data not shown), making them a valid control. In both βPS^{-} and control embryos, peak pMad levels increase markedly between stage 5 and stage 6 (Figure 1E), consistent with previous reports of pMad gradient dynamics (Rushlow et al., 2001). At stage 5, pMad levels are considerably lower in βPS^{-} embryos than controls, resulting in a narrower gradient and a reduced peak (Figure 1E). At stage 6, peak pMad levels at the dorsal midline reach similar levels in βPS^{-} and control embryos (Figure 1E); however, the dorsal domains over which the gradient reaches a threshold of 0.4 and 0.6 are significantly narrower (Figures 1F and 1G). In wild-type embryos, these thresholds correspond to the width of *ush* (~14 cells; see Figure 1A) and *Race/hnt* (four to six cells; see Figure 3D) expression, respectively, consistent with the reduction in pMad levels leading to disrupted BMP target gene expression in βPS^{-} embryos. Although we cannot rule out additional effects on non-canonical BMP signal transduction or BMP-independent effects, our data demonstrate that integrins are required for the timely and robust formation of the pMad gradient in the early embryo.

The Signaling Function of Integrins Is Sufficient for Their Role in BMP Pathway Activation

To test if integrins exert their effect on BMP signaling through their extracellular ligand binding activity or by activating intracellular signaling pathways, we made use of a chimeric receptor, $Torso^{D}\beta PS_{cyt}$, in which the cytoplasmic domain of βPS is fused to the transmembrane and extracellular domains of a constitutively active form of the Torso receptor (Martin-Bermudo and Brown, 1999). This integrin signaling construct is unable to bind integrin ligands, but it is capable of signaling due to $Torso^{D}$-mediated clustering of the βPS cytoplasmic domain (Figure 2A). We used the Gal4/UAS-system to express wild-type βPS or $Torso^{D}\beta PS_{cyt}$ transgenes in βPS^{-} embryos and tested for their ability to rescue the BMP phenotype. Zygotic expression of wild-type βPS restores *Race* expression in ~50% of embryos (Figure 2B). Rescue in only half of the embryos likely reflects the proportion expressing the Gal4 transcription factor maternally and zygotically, as opposed to maternally only. The $Torso^{D}\beta PS_{cyt}$ integrin signaling construct was also able to rescue *Race* and *hnt* induction in βPS^{-} embryos (Figures 2B and 2C), demonstrating that the signaling function of integrins is sufficient for their role in promoting BMP signaling. Overexpression of βPS or $Torso^{D}\beta PS_{cyt}$ in a wild-type background does not broaden *Race* or *hnt* expression (Figure S3), suggesting that whereas integrin signaling is required to augment BMP signaling, it is not limiting with respect to this function in a wild-type context. We conclude that integrin signaling is permissive for generating peak levels of BMP pathway activation.

Integrin Signaling Acts Downstream of Collagen IV to Enhance BMP Activity

We have shown previously that collagen IV mutant embryos have disrupted BMP signaling due to an altered extracellular BMP distribution (Wang et al., 2008). If collagen IV acts as an integrin ligand, a loss of integrin signaling may contribute to the defect in BMP signaling observed in collagen IV mutant embryos (Figure 3A). To test this, we examined whether $Torso^{D}\beta PS_{cyt}$, which induces integrin signaling independent of ECM ligands, can rescue BMP target gene expression in embryos with reduced levels of collagen IV (Figure 3A), due to a mutation in *viking*, one of two collagen IV genes in *Drosophila* (Wang et al., 2008). As shown in Figure 3B, overexpression of $Torso^{D}\beta PS_{cyt}$ restores *Race* induction in ~50% of embryos, whereas wild-type βPS, which requires an ECM ligand for activation of signaling, has no effect. This result suggests that integrin signaling may act downstream of collagen IV to enhance BMP activity. The partial rescue of *Race* expression observed with $Torso^{D}\beta PS_{cyt}$ in

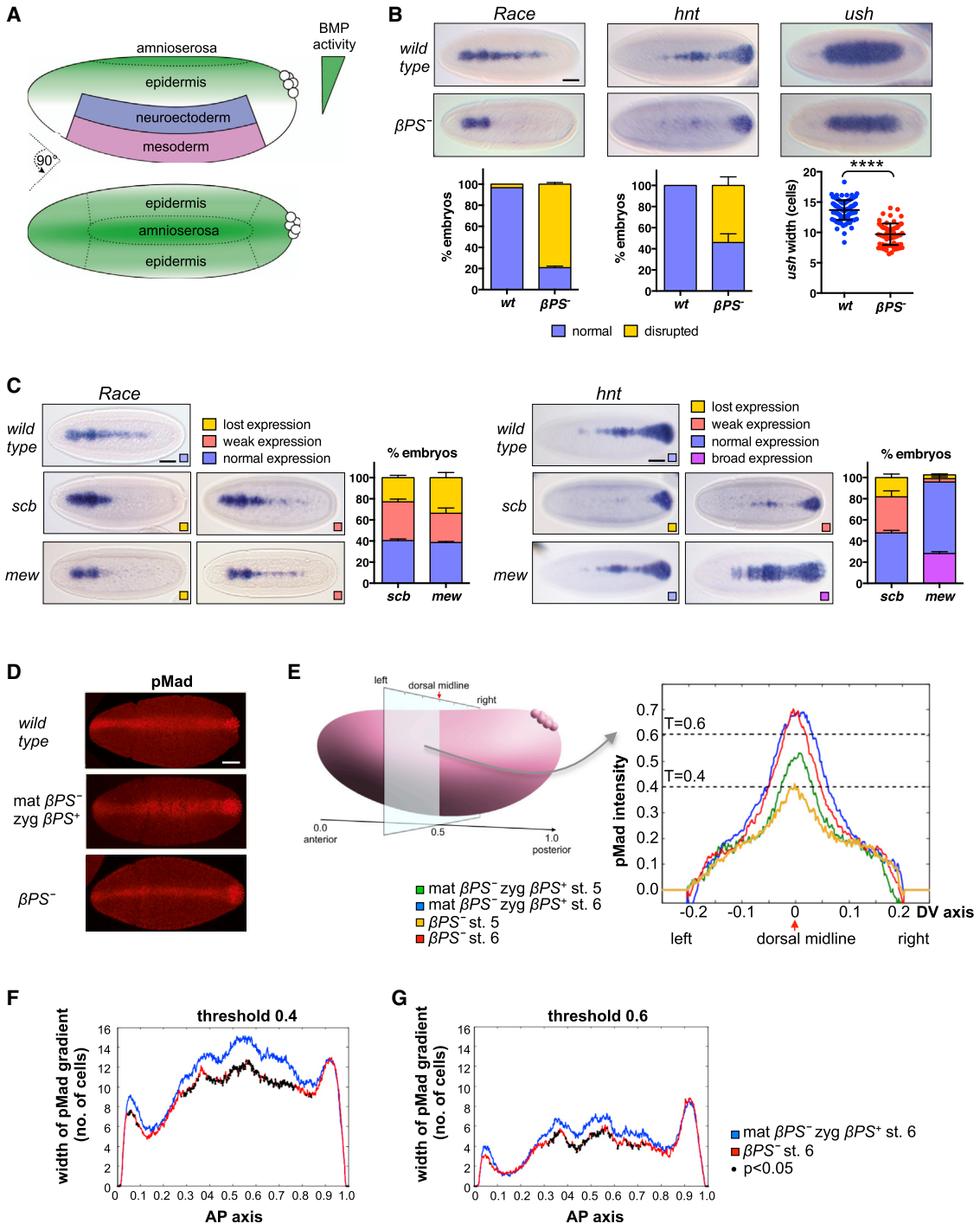

Figure 1. Loss of Integrin Expression Causes Defects in BMP Signaling Responses in the Early Embryo

(A) Early *Drosophila* embryo showing patterning of the dorsal ectoderm by a gradient of BMP activity.

(B) RNA in situ hybridizations of wild-type or maternal/zygotic mys^{XG43} mutant (βPS^{-}) embryos showing expression of the BMP target genes *Race*, *hnt*, and *ush*. For *Race* and *hnt* quantification, n = 3, >15 embryos per genotype in each experiment; error bars represent SEM. For *ush* width, individual measurements are shown with mean ± SD (n = 92 for wild-type and n = 69 for βPS^{-}). ****p < 0.0001 (unpaired t test).

(C) RNA in situ hybridizations for *Race* and *hnt* in *mew* (mew^{M6}) and *scb* (scb^{5J38}) mutant embryos. Phenotypes were classified as "lost," "weak," or "broad" (see Supplemental Experimental Procedures and Figure S2B for details) and were counted on embryo samples collected from heterozygous mutant stocks (n = 3, >60 embryos counted per genotype in each experiment; error bars represent SEM).

(D) pMad immunostaining of wild-type, maternal βPS^{-} zygotic βPS^{+} (mat βPS^{-} zyg βPS^{+}) and maternal/zygotic βPS^{-} (βPS^{-}) embryos. All scale bars represent 50 μm.

(legend continued on next page)

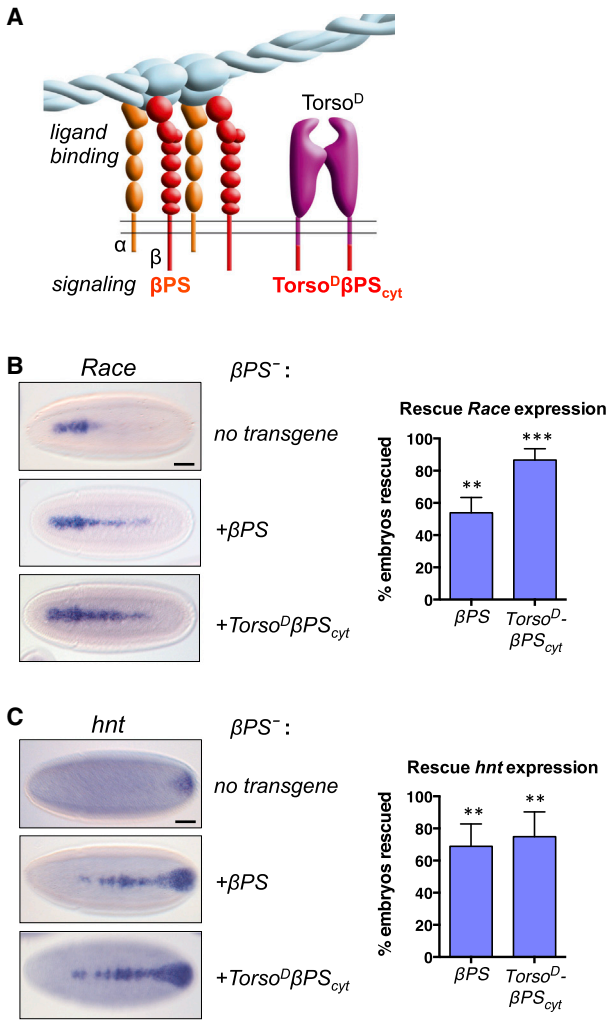

Figure 2. Integrin Signaling Is Sufficient to Rescue the BMP Phenotype in *βPS*⁻ Integrin Mutant Embryos

(A) Torso^{D}βPS$_{cyt}$ construct, which can mimic integrin signaling in the absence of ligand binding.

(B and C) Overexpression of βPS and of Torso^{D}βPS$_{cyt}$ in maternal/zygotic *mys*^{XG43} mutant (*βPS*⁻) embryos can rescue expression of the peak threshold BMP target genes *Race* (B) and *hnt* (C). Rescue was quantified as the percentage increase in embryos with a wild-type expression pattern relative to a no transgene control (n = 3, > 50 embryos counted per genotype in each experiment; error bars are SEM). For details, see Supplemental Experimental Procedures. Asterisks denote significant difference from no transgene control (i.e., 0% rescue); **p < 0.01, ***p < 0.001 (t test). Scale bars represent 50 μm. See also Figure S3.

collagen IV mutant embryos, as compared to *βPS*⁻ embryos (Figure 2B), is consistent with a dual role for collagen IV in promoting BMP signaling in the early embryo: to activate integrin signaling and promote extracellular BMP gradient formation (Sawala et al., 2012; Wang et al., 2008). In agreement with this, a reduction in collagen IV leads to a more severe decrease in BMP signaling than the loss of integrins, based on the width of *ush* expression (Figure 3C).

To exclude the possibility that the loss of integrin signaling in collagen IV mutants is due to a general loss of ECM integrity, we examined BMP signaling in embryos lacking expression of laminin, an ECM protein that interacts with the collagen IV network and can act as an integrin ligand in *Drosophila* (Brown, 2000). In contrast to integrin and collagen IV mutants, embryos lacking β-laminin show a variable expansion of the *Race* expression domain (Figure 3D). We speculate that this expanded *Race* expression is due to competition between collagen IV and laminin for binding to integrins, with only collagen IV interactions leading to BMP-promoting signaling events. In support of this, we find that addition of laminin to *Drosophila* cells plated on a collagen IV substrate, but not when plated on plastic, inhibits pMad accumulation in a dose-dependent manner following pathway stimulation, and this effect is reduced by co-transfecting additional βPS (Figure 3E, right panel). Together, these results suggest that engagement of integrin receptors by collagen IV, but not laminin, promotes BMP responses in the early *Drosophila* embryo.

Integrin Signaling Acts Downstream of BMP Receptor Activation to Enhance pMad Accumulation

We next investigated the molecular link between integrin signaling and enhanced BMP signal transduction. A key signaling protein linking integrin to growth factor pathways is focal adhesion kinase (FAK) (Giancotti and Ruoslahti, 1999). However, we did not detect any defect in BMP signaling in embryos lacking *Drosophila* FAK (Figure S4A), suggesting that integrin signaling enhances BMP signal transduction through an FAK-independent mechanism.

To further dissect this mechanism, we developed a *Drosophila* tissue culture assay. Treatment of S2R+ cells with the BMP ligand Dpp induces pMad, and this is enhanced when cells are plated on collagen IV (Figure 4A). RNAi-mediated knockdown of βPS abolishes the stimulatory effect of collagen IV on pMad induction, whereas it has no effect on pMad levels in plastic-plated cells (Figures 4A and 4C). As shown in Figures 4B and 4C, βPS RNAi in collagen IV-plated cells also reduces pMad induction by a constitutively active form of the BMP receptor Thickveins (Tkv), Tkv^{QD}, indicating that collagen IV/integrin signaling acts downstream of Tkv activation. The effects of collagen IV/integrins on pMad levels do not coincide with changes in the levels of total Mad (transfected Flag-Mad) (Figures 4A and 4B), suggesting that they are not mediated via an effect on Mad stability. In terms of the α-integrin requirement, knockdown of both *mew* and *scb* together, but not either subunit alone, also reduces pMad accumulation (Figure 4D), suggesting that both α-integrins can function with βPS to stimulate pMad.

(E–G) Quantification of the pMad gradient in mat *βPS*⁻, zyg *βPS*$^{+}$, and *βPS*⁻ embryos. (E) Mean pMad intensity along the dorsal-ventral axis at 0.5 embryo length. Threshold lines indicate the width of the pMad gradient plotted in (C) and (D). (F and G) Mean width of the pMad gradient at thresholds 0.4 (C) and 0.6 (D) along the anterior-posterior axis for stage 6 embryos. Black dots indicate significant differences (p < 0.05) between maternal *βPS*⁻ zyg *βPS*$^{+}$ and *βPS*⁻.

All embryo images show dorsal views of stage 6 embryos, anterior to the left. See also Figures S1 and S2.

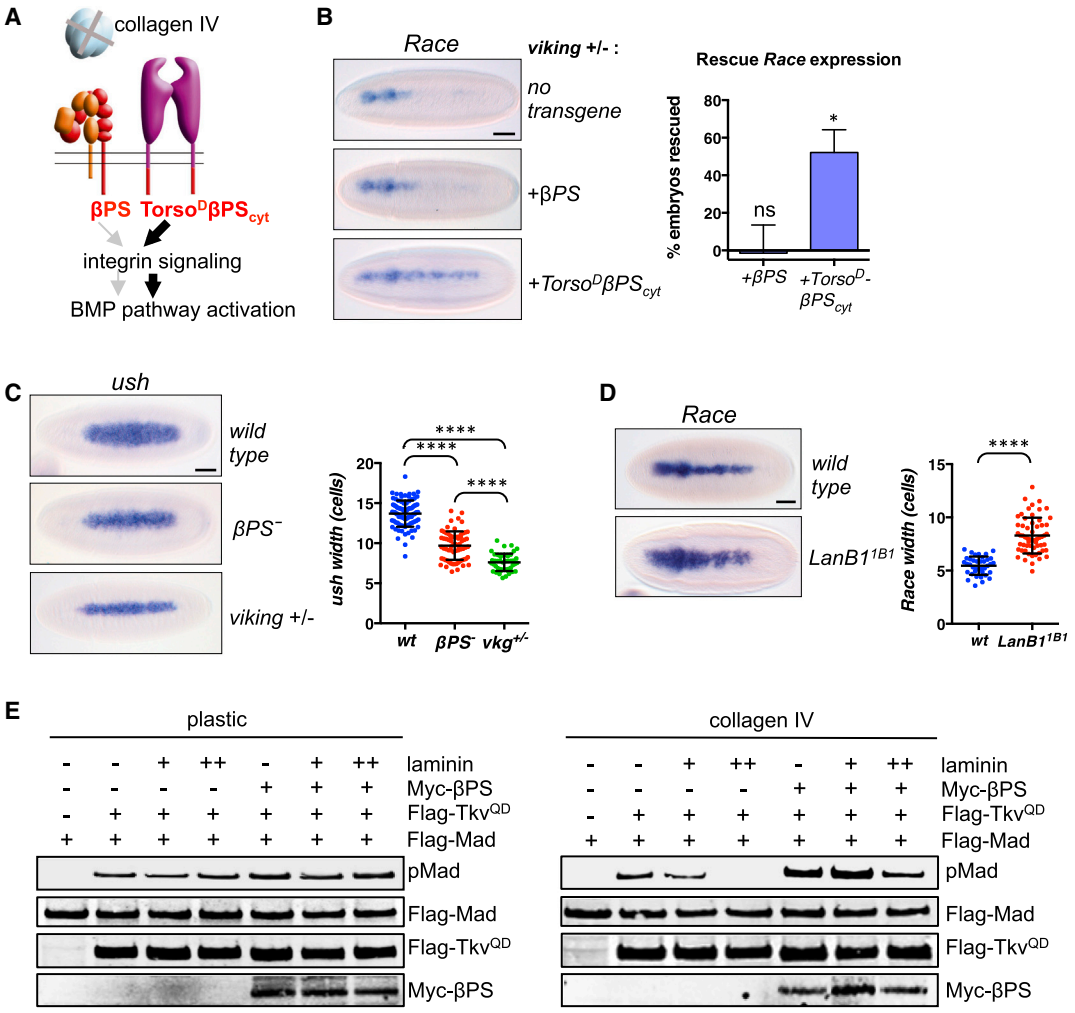

Figure 3. Activation of Integrin Signaling Can Partially Restore BMP Signaling Defects in Collagen IV Mutant Embryos

(A) Diagram showing how a potential loss of integrin signaling in collagen IV mutant embryos may reduce BMP signaling (left), which would be predicted to be rescued by constitutively active integrin signaling (right).

(B) Expression of Torso^{D}βPS$_{cyt}$, but not wild-type βPS, can partially restore expression of *Race* in collagen IV (*viking*) mutant embryos. *Race* expression patterns were classified as normal, weak, or lost (n = 3, >70 embryos counted per genotype in each experiment; error bars represent SEM). Asterisks denote significant difference from no transgene control (i.e., 0% rescue); *p < 0.05 (t test). See Supplemental Experimental Procedures for details of rescue quantification.

(C) The *ush* expression pattern is narrower in collagen IV (*viking*) mutant embryos than in embryos lacking β integrin (*βPS*$^{-}$). *ush* width shown as individual measurements and mean ± SD, n > 45 for each genotype; ****p < 0.0001 (ordinary one-way ANOVA).

(D) Maternal/zygotic *LanB1*^{1B1} mutant embryos show a broadened *Race* expression pattern. *Race* width shown as individual measurements and mean ± SD, n > 35 for each genotype; ****p < 0.0001 (Welch's test). Scale bars represent 50 μm.

(E) Western blot of pMad and transfected Flag-Mad (total Mad), Flag-Tkv^{QD}, and Myc-βPS in S2R+ cells which were plated on either plastic or collagen IV and treated with increasing levels of laminin, as indicated.

Consistent with our in vivo rescue experiments (Figures 2 and 3), the positive effect of collagen IV/integrins on both Dpp- or Tkv^{QD}-induced pMad accumulation can be mimicked by expression of Torso^{D}βPS$_{cyt}$ (Figures 4E and 4F), confirming that integrin signaling mediates the effect on pMad observed in S2R+ cells and demonstrating that integrin signaling acts cell autonomously to enhance BMP responses. We next used the Torso^{D}βPS$_{cyt}$ construct to identify residues in the βPS cytoplasmic domain required for integrin-enhanced pMad accumulation. Two conserved NPXY motifs in the β-integrin cytoplasmic tail are important for the recruitment of a variety of integrin-binding proteins (Legate et al., 2009). Mutation of tyrosine in the first (Y831) or second (Y843) NPXY motif to alanine, either alone or in combination, did not affect expression levels of Torso^{D}βPS$_{cyt}$ (Figure 4F) but compromised its ability to promote pMad phosphorylation (Figure 4F). These results suggest that both NPXY motifs in the βPS cytoplasmic tail are important for its enhancement of BMP signaling.

To gain further mechanistic insight, we tested if integrin receptors interact with Tkv. Indeed, we found that Tkv, but not a

control transmembrane protein (Frizzled), can co-immunoprecipitate with βPS, *mew* (αPS1) and *scb* (αPS3) (Figures 4G–4I). The interaction between αPS1 or αPS3 and Tkv is abrogated by βPS RNAi (Figures 4H and 4I), consistent with integrin surface presentation being dependent on functional integrin receptors (Leptin et al., 1989). We next truncated the βPS cytoplasmic tail after residues involved in stabilization of the integrin α-β heterodimer (Figure S4B). A similar truncation in mammalian β3 integrin does not disrupt cell-surface expression (O'Toole et al., 1991), a result we confirmed for our βPS-trunc construct (Figure S4C). As shown in Figure 4J, truncation of the βPS cytoplasmic tail abrogates the interaction with Tkv, suggesting that the integrin-Tkv interaction is mediated intracellularly and therefore could be relevant for the integrin-mediated enhancement of Tkv-mediated Mad phosphorylation. By contrast, mutation of the NPXY motifs in the βPS did not impair its binding to Tkv (Figure 4J). As the NPXY motifs are required for integrin-signaling mediated enhancement of pMad (Figure 4F), this suggests that binding of integrins to Tkv alone is not sufficient to enhance pMad accumulation (see Discussion). Together, our data suggest that integrin receptors can form complexes with BMP receptors, enhancing their ability to phosphorylate Mad.

The α-Integrin Subunit scb/αPS3 Is Itself a BMP Target Gene

The spatial and temporal expression pattern of *scb* is consistent with this α-integrin encoding gene being positively regulated by BMP signaling. Therefore we examined the *scb* expression pattern in embryos with increased and decreased levels of BMP signaling. We found that *scb* expression is expanded ventrally in embryos with four copies of *dpp* or overexpressing the activated BMP receptor, tkv^{QD}, and lost in dpp^{Hin37} mutant embryos (Figure 5A). The lack of *scb* expression in the central region of the embryo can be explained at least in part by a repressive input from the gap gene transcription factor Krüppel, as *scb* expression expands into the central region in *Krüppel* mutant embryos (Figure S5). Overall, these data demonstrate that *scb* is indeed a BMP target gene and identify a positive feedback loop in which BMP-dependent induction of *scb* expression further enhances BMP signal transduction via the activation of integrin signaling.

DISCUSSION

Our study reveals that BMP-responsive transcription during *Drosophila* embryonic dorsal-ventral axis patterning is not simply a readout of the BMP signal but instead requires synergy between BMP and integrin signaling. Our data support a model whereby collagen IV activation of integrin signaling augments pMad levels (Figure 5B). Consistent with collagen IV acting as an integrin ligand, which is well documented in vertebrates (Khoshnoodi et al., 2008), collagen-IV-directed rotations of follicle epithelia during *Drosophila* oogenesis also require integrins (Haigo and Bilder, 2011). Thus, we envisage two functions for collagen IV in regulating BMP signaling (Figure 5B): (1) collagen IV shapes the BMP gradient through a direct collagen IV-Dpp interaction, as we have described previously (Sawala et al., 2012; Wang et al., 2008); and (2) collagen IV activates integrin signaling, which amplifies the BMP signal by forming complexes with BMP receptors and enhancing induction of pMad. In addition, we show specificity for collagen-IV-induced integrin activation, as laminin, which can bind both αPS1- and αPS3-containing integrin receptors (Brown, 2000; Schöck and Perrimon, 2003), does not promote BMP responses, possibly due to activation of a distinct signaling complex that does not increase pMad. Instead, our data support competition between collagen IV and laminin for integrin binding, suggesting that the relative levels of laminin, collagen IV, and integrins in a particular developmental context will impact the extent of BMP pathway activation.

Mechanism of Integrin-Enhanced BMP Signal Transduction

Our data indicate that collagen IV/integrin signaling in the early embryo promotes activation of canonical Smad-dependent signal transduction in a mechanism that is independent of FAK but may involve an association of integrins and BMP receptors. Several recent studies have also reported interactions between integrins and BMP receptors, leading to inhibition of Smad phosphorylation (North et al., 2015) or enhanced Smad phosphorylation either via a BMP-ligand-independent, shear-stress-induced activation of FAK/ERK MAPK signaling (Zhou et al., 2013) or via extracellular domain interactions that increase the ligand binding affinity of the BMP receptor (Tian et al., 2012). Our data show that collagen IV/integrin signaling enhances pMad levels via a distinct mechanism, as it is independent of FAK and involves intracellular domain interactions downstream of BMP receptor activation.

We identify two conserved NPXY motifs in the βPS cytoplasmic domain as important sites for integrin-BMP synergy, but these motifs are not required for βPS binding to Tkv, suggesting that binding of integrins to BMP receptors is not sufficient for promoting Mad phosphorylation. One possibility is that the NPXY motifs are required for the recruitment of factors that facilitate or stabilize Mad phosphorylation. NPXY motifs are also involved in regulating the endocytosis and recycling of integrin receptors (Margadant et al., 2012). As some evidence suggests that Smad phosphorylation by BMP receptors occurs preferentially on endosomes (Shi et al., 2007), integrin-facilitated endocytosis and/or recycling of BMP receptors could enhance Mad phosphorylation.

Roles of αPS1/mew and αPS3/scb in Integrin-Mediated Enhancement of BMP Signaling

Previously, integrins have been implicated in regulating Sog distribution in ovarian follicle cells and the pupal wing (Araujo et al., 2003; Negreiros et al., 2010). Although the low penetrance *sog* mutant-like phenotype we observed in *mew* mutant embryos is also consistent with a function of *mew*/αPS1 in modulating Sog levels (Figure 5B), the major role of integrins in the early embryo appears to involve their signaling function, as we can rescue the integrin-null phenotype with the $Torso^{D}βPS_{cyt}$ signaling-activated transgene. Consistent with this, our RNAi knockdown data suggest that integrin signaling through both αPS1 and αPS3 can promote Tkv-mediated Mad phosphorylation and both αPS1 and αPS3 bind Tkv. In the early embryo,

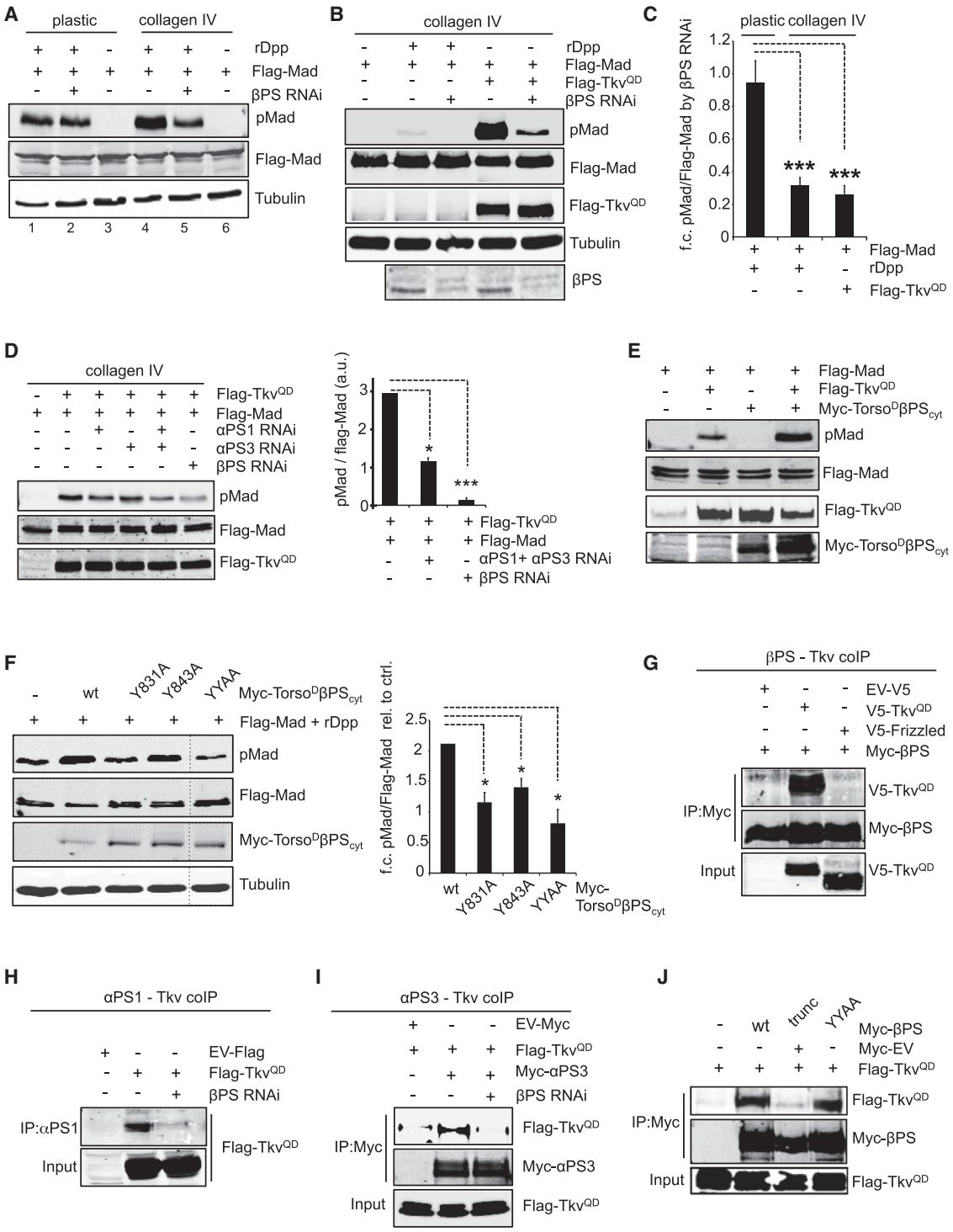

Figure 4. Molecular Mechanism of Integrin-Signaling-Mediated Enhancement of the BMP Pathway

(A) Western blot for Flag-Mad, pMad, and tubulin in S2R+ cells transfected with Flag-Mad, which were plated on either plastic or collagen IV and treated with rDpp and βPS RNAi, as indicated.

(B) Western blot for Flag-Mad, pMad, Flag-Tkv^{QD}, βPS, and tubulin in cells transfected with Flag-Mad and plated on collagen IV. BMP signaling was activated by co-transfection of Flag-Tkv^{QD} or treatment with rDpp, and cells were treated with βPS RNAi as indicated.

(C) Quantification of the experiments in (A) and (B), showing fold reduction in pMad activation by βPS RNAi on plastic- or collagen-IV-plated cells. pMad levels were normalized to total Mad (Flag-Mad) in each sample. n = 3–6; ***$p < 0.001$ (one-way ANOVA).

(legend continued on next page)

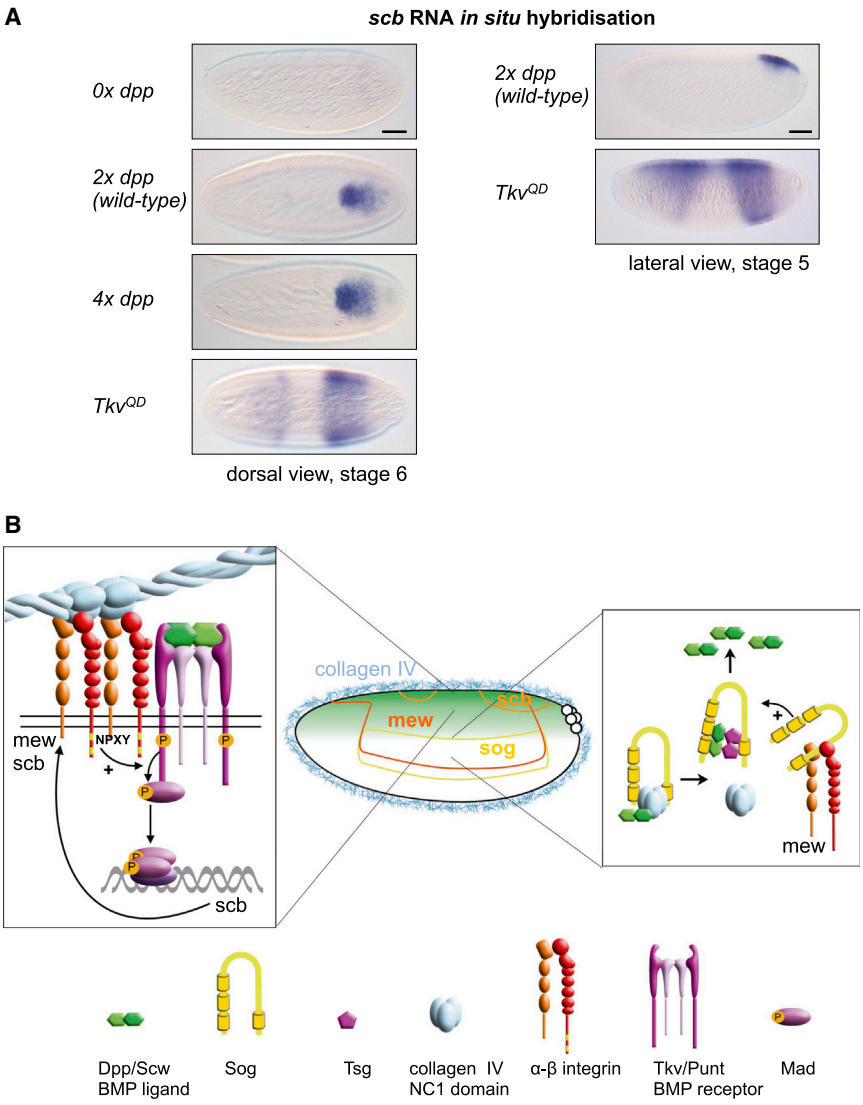

Figure 5. A Positive Feedback Loop Potentiates Integrin-BMP Synergy

(A) RNA in situ hybridizations for *scb* in wild-type embryos and in embryos with altered levels of BMP signaling. Scale bars represent 50 μm.

(B) Model of integrin-BMP synergy. See Discussion for details.

See also Figure S5.

due to their different expression patterns and their distinct additional roles of promoting Sog function (αPS1) or providing positive feedback on BMP signaling (αPS3), we expect αPS1 and αPS3 to act only partially redundantly. Indeed, we observe disrupted BMP target gene expression in *mew* and *scb* single mutants, with distinct spatial pattern of *Race* defects. As BMP target gene expression in the central region of the embryo (expressing only αPS1) is more sensitive than the regions in the anterior and posterior (expressing both αPS1 and αPS3) to genetic perturbations, such as overexpression of Sog (Winstanley et al., 2015), we speculate that integrin signaling through both αPS1 and αPS3 may contribute to robustness of the pMad gradient in vivo.

Integrin Signaling as a Positive Feedback Loop for BMP Activity

Our data reveal that expression of *scb* is induced by BMP signaling in the early embryo, identifying a positive feedback loop in which activation of *scb* allows integrin signaling, which further increases BMP responses at the dorsal midline. Positive feedback, involving a transcriptional mechanism, has previously been implicated in the conversion of the BMP activity gradient into a spatially bistable pattern of gene expression that subdivides the dorsal ectoderm into distinct tissues (Wang and Ferguson, 2005). Recently, the tumor necrosis factor α ligand *eiger* has been identified in the positive feedback circuit, but additional genes are thought to be involved (Gavin-Smyth et al., 2013). *scb* may represent such an additional BMP target gene.

In summary, our findings reveal that interpretation of the BMP embryonic morphogen gradient requires not only a response to the extracellular BMP concentration but also integrin-mediated enhancement through positive feedback and integration of context-specific information from the ECM. We predict that the integrin-BMP synergy identified here may have wide-ranging implications during other development or disease contexts where the functions of BMPs, collagen IV, and integrins converge, such as stem cell fate decisions or angiogenesis.

(D) Western blot as described in (B) with quantitation, but cells were also treated with αPS1 and/or αPS3 RNAi.

(E) Western blot for Flag-Mad, pMad, Flag-Tkv^{QD}, and Myc-Torso^{D}βPS$_{cyt}$ in cells transfected with Flag-Mad, Flag-Tkv^{QD}, and Myc-Torso^{D}βPS$_{cyt}$ and plated on plastic.

(F) As in (E), except cells were transfected with Flag-Mad and Myc-tagged wild-type or mutant Torso^{D}βPS$_{cyt}$, and treated with rDpp. Quantitation shows increase in pMad (n = 4); *p < 0.05, **p < 0.001 (paired t tests).

(G–I) Co-immunoprecipitation experiments between Flag-Tkv^{QD} and the βPS (G), αPS1 (H), and αPS3 (I) integrin subunits. Frizzled is a negative control.

(J) Co-immunoprecipitation between Flag-Tkv^{QD} and Myc-βPS forms with truncation of the cytoplasmic tail or both NPXY motifs mutated.

All error bars show SEM. See also Figure S4.

EXPERIMENTAL PROCEDURES

Fly Strains, Crosses, Embryo Collection, and Phenotype Analysis

Embryos were collected, aged, and fixed with formaldehyde using standard procedures. Details of fly strains, crosses, and phenotype analysis are provided in Supplemental Experimental Procedures.

RNA In Situ Hybridization and Immunostaining

RNA in situ hybridizations were performed using digoxigenin-UTP-labeled exonic RNA probes. Fluorescent RNA in situ hybridizations were performed as previously described (Kosman et al., 2004) using digoxigenin-UTP-labeled probes for exon 5 of *mew* and full-length *sog* and a biotin-UTP-labeled probe for exon 3 of *scb*. Antibodies used were sheep anti-digoxigenin (1:400, Roche), mouse anti-biotin (1:400, Invitrogen), donkey anti-mouse-immunoglobulin G (IgG)-Alexa 488 (1:500, Invitrogen), and donkey anti-sheep-IgG-Alexa 555 (1:500, Invitrogen). For immunostaining, antibodies used were rabbit anti-pMad (1:250, gift from P. ten Dijke), chicken anti-β-Gal (1:1,000, Abcam), anti-rabbit-IgG-Alexa 594 (1:400, Invitrogen), and anti-chicken-IgG-488 (1:400, Invitrogen). Immunostained embryos were mounted in Prolong (Invitrogen). Detailed protocols are available on request. For details of pMad quantification, see Supplemental Experimental Procedures.

Drosophila S2 Cell Culture Experiments

Drosophila S2R+ cells were cultured at 25°C in insect medium (PAA Laboratories) with 10% FBS (PAA Laboratories) and 1% penicillin/streptomycin, plated on human collagen IV or plastic, and transiently transfected using Effectene (QIAGEN). Where appropriate, expression was induced with 500 μM $CuSO_4$ 24 hr post-transfection. Cells were harvested 72h after transfection or Cu-induction and lysed in NP40 buffer (150 nM NaCl, 20 mM Tris-Cl [pH 8], 1% NP-40, EDTA, 0.1% protease and phosphatase inhibitor) for SDS-PAGE/western blotting. For RNAi treatment, cells were serum-starved for 1 hr and treated with 10 μg/ml double-stranded RNA for 2 hr at 25°C, then 10% FBS was added to the medium. For stimulation with Dpp, transfected cells were serum-starved for 1 hr, followed by addition of 3 nM recombinant Dpp (rDpp) (R&D Systems) for 2 hr before lysis. Protein bands were quantified using Li-COR Imager (Li-COR Biosciences) and ImageJ. For details of DNA transfections, collagen IV plating, laminin competition, co-immunoprecipitation, and immunofluorescence experiments, see Supplemental Experimental Procedures.

SUPPLEMENTAL INFORMATION

Supplemental Information includes Supplemental Experimental Procedures and five figures and can be found with this article online at http://dx.doi.org/10.1016/j.celrep.2015.08.012.

AUTHOR CONTRIBUTIONS

A.S. designed and performed in vivo experiments, analyzed the data, and wrote the manuscript. M.S. performed tissue culture experiments and analyzed the data. C.S. generated some DNA/RNA reagents and performed some in situ hybridizations. S.G.W. performed fluorescent in situ hybridization experiments. H.L.A. designed experiments, analyzed the data, and wrote the manuscript.

ACKNOWLEDGMENTS

We thank David Umulis (Purdue University) for the pMad quantification and Pat Caswell for helpful discussions. We also thank Nick Brown, Ruth Palmer, Norbert Perrimon, Peter ten Dijke, and Jean-Paul Vincent for DNA, antibodies, or fly stocks; Lisa Deignan for providing *dpp* mutant and tkv^{QD}-overexpressing embryos; and Victoria Coyne for providing *Kr* mutant embryos. This work was supported by a Wellcome Trust program grant to H.L.A. (092005/Z/10/A) and a Wellcome Trust PhD studentship to A.S. (083271/Z/07/Z).

Received: March 20, 2015
Revised: June 19, 2015
Accepted: August 4, 2015
Published: August 27, 2015

REFERENCES

Alam, N., Goel, H.L., Zarif, M.J., Butterfield, J.E., Perkins, H.M., Sansoucy, B.G., Sawyer, T.K., and Languino, L.R. (2007). The integrin-growth factor receptor duet. J. Cell. Physiol. *213*, 649–653.

Araujo, H., Negreiros, E., and Bier, E. (2003). Integrins modulate Sog activity in the Drosophila wing. Development *130*, 3851–3864.

Brown, N.H. (2000). Cell-cell adhesion via the ECM: integrin genetics in fly and worm. Matrix Biol. *19*, 191–201.

Bunt, S., Hooley, C., Hu, N., Scahill, C., Weavers, H., and Skaer, H. (2010). Hemocyte-secreted type IV collagen enhances BMP signaling to guide renal tubule morphogenesis in Drosophila. Dev. Cell *19*, 296–306.

Gavin-Smyth, J., Wang, Y.-C., Butler, I., and Ferguson, E.L. (2013). A genetic network conferring canalization to a bistable patterning system in Drosophila. Curr. Biol. *23*, 2296–2302.

Giancotti, F.G., and Ruoslahti, E. (1999). Integrin signaling. Science *285*, 1028–1032.

Haigo, S.L., and Bilder, D. (2011). Global tissue revolutions in a morphogenetic movement controlling elongation. Science *331*, 1071–1074.

Hynes, R.O. (2009). The extracellular matrix: not just pretty fibrils. Science *326*, 1216–1219.

Khoshnoodi, J., Pedchenko, V., and Hudson, B.G. (2008). Mammalian collagen IV. Microsc. Res. Tech. *71*, 357–370.

Kosman, D., Mizutani, C.M., Lemons, D., Cox, W.G., McGinnis, W., and Bier, E. (2004). Multiplex detection of RNA expression in Drosophila embryos. Science *305*, 846.

Legate, K.R., Wickström, S.A., and Fässler, R. (2009). Genetic and cell biological analysis of integrin outside-in signaling. Genes Dev. *23*, 397–418.

Leptin, M., Bogaert, T., Lehmann, R., and Wilcox, M. (1989). The function of PS integrins during Drosophila embryogenesis. Cell *56*, 401–408.

Margadant, C., Kreft, M., de Groot, D.J., Norman, J.C., and Sonnenberg, A. (2012). Distinct roles of talin and kindlin in regulating integrin α5β1 function and trafficking. Curr. Biol. *22*, 1554–1563.

Martin-Bermudo, M.D., and Brown, N.H. (1999). Uncoupling integrin adhesion and signaling: the betaPS cytoplasmic domain is sufficient to regulate gene expression in the Drosophila embryo. Genes Dev. *13*, 729–739.

Negreiros, E., Fontenele, M., Câmara, A.R., and Araujo, H. (2010). alphaPS1-betaPS integrin receptors regulate the differential distribution of Sog fragments in polarized epithelia. Genesis *48*, 31–43.

North, H.A., Pan, L., McGuire, T.L., Brooker, S., and Kessler, J.A. (2015). β1-Integrin alters ependymal stem cell BMP receptor localization and attenuates astrogliosis after spinal cord injury. J. Neurosci. *35*, 3725–3733.

O'Toole, T.E., Mandelman, D., Forsyth, J., Shattil, S.J., Plow, E.F., and Ginsberg, M.H. (1991). Modulation of the affinity of integrin alpha IIb beta 3 (GPIIb-IIIa) by the cytoplasmic domain of alpha IIb. Science *254*, 845–847.

Paralkar, V.M., Weeks, B.S., Yu, Y.M., Kleinman, H.K., and Reddi, A.H. (1992). Recombinant human bone morphogenetic protein 2B stimulates PC12 cell differentiation: potentiation and binding to type IV collagen. J. Cell Biol. *119*, 1721–1728.

Rushlow, C., Colosimo, P.F., Lin, M.C., Xu, M., and Kirov, N. (2001). Transcriptional regulation of the Drosophila gene zen by competing Smad and Brinker inputs. Genes Dev. *15*, 340–351.

Sawala, A., Sutcliffe, C., and Ashe, H.L. (2012). Multistep molecular mechanism for bone morphogenetic protein extracellular transport in the Drosophila embryo. Proc. Natl. Acad. Sci. USA *109*, 11222–11227.

Schöck, F., and Perrimon, N. (2003). Retraction of the Drosophila germ band requires cell-matrix interaction. Genes Dev. *17*, 597–602.

Shi, W., Chang, C., Nie, S., Xie, S., Wan, M., and Cao, X. (2007). Endofin acts as a Smad anchor for receptor activation in BMP signaling. J. Cell Sci. *120*, 1216–1224.

Tian, H., Mythreye, K., Golzio, C., Katsanis, N., and Blobe, G.C. (2012). Endoglin mediates fibronectin/α5β1 integrin and TGF-β pathway crosstalk in endothelial cells. EMBO J. *31*, 3885–3900.

Umulis, D.M., Shimmi, O., O'Connor, M.B., and Othmer, H.G. (2010). Organism-scale modeling of early Drosophila patterning via bone morphogenetic proteins. Dev. Cell *18*, 260–274.

Wang, Y.C., and Ferguson, E.L. (2005). Spatial bistability of Dpp-receptor interactions during Drosophila dorsal-ventral patterning. Nature *434*, 229–234.

Wang, X., Harris, R.E., Bayston, L.J., and Ashe, H.L. (2008). Type IV collagens regulate BMP signalling in Drosophila. Nature *455*, 72–77.

Winstanley, J., Sawala, A., Baldock, C., and Ashe, H.L. (2015). Synthetic enzyme-substrate tethering obviates the Tolloid-ECM interaction during Drosophila BMP gradient formation. eLife *4*, e05508.

Wu, M.Y., and Hill, C.S. (2009). Tgf-beta superfamily signaling in embryonic development and homeostasis. Dev. Cell *16*, 329–343.

Zhou, J., Lee, P.L., Lee, C.I., Wei, S.Y., Lim, S.H., Lin, T.E., Chien, S., and Chiu, J.J. (2013). BMP receptor-integrin interaction mediates responses of vascular endothelial Smad1/5 and proliferation to disturbed flow. J. Thromb. Haemost. *11*, 741–755.

Cell Reports

Supplemental Information

Peak BMP Responses in the *Drosophila* Embryo Are Dependent on the Activation of Integrin Signaling

Annick Sawala, Margherita Scarcia, Catherine Sutcliffe, Scott G. Wilcockson, and Hilary L. Ashe

Supplemental Figures

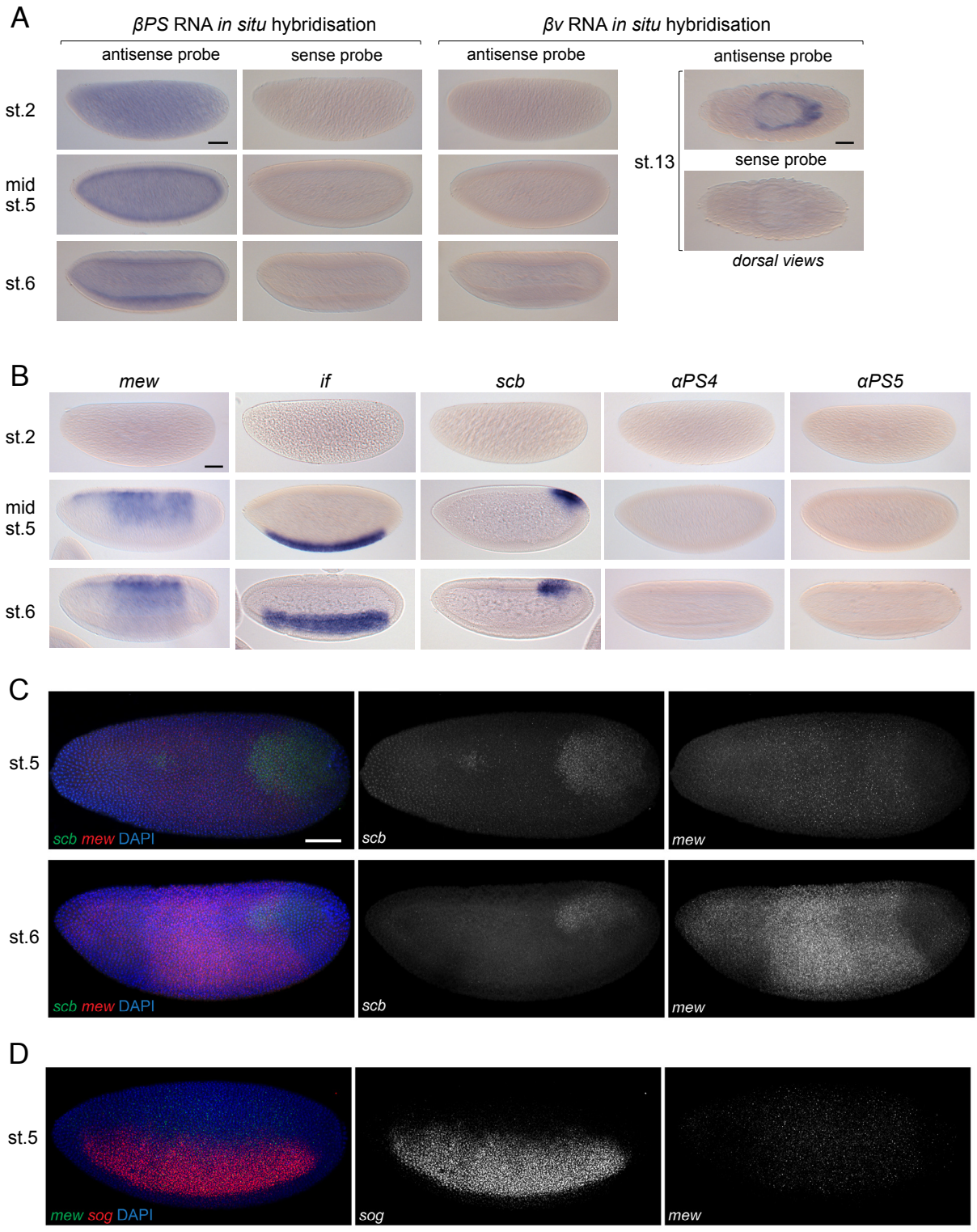

Figure S1, related to Figure 1: Expression of integrin genes during early *Drosophila* embryogenesis. RNA *in situ* hybridisations of early embryos (pre-cellularisation, stage 2; mid-cellularisation, stage 5; early gastrulation, stage 6) to visualise expression of α-integrin and β-integrin genes present in *Drosophila*. Note that transcripts detected in stage 2 embryos are maternally inherited. All images are lateral views, anterior to the left, unless otherwise stated. Scale bars = 50 μm.

(A) RNA *in situ* hybridisation for the two β-integrin genes present in *Drosophila*, *βPS* and *βv* (Brown, 2000). *βPS* is expressed maternally and in blastula/gastrula stages, with a ubiquitous expression pattern at all stages. *βv* expression is not detected in early embryos. Stage 13 embryos, where *βv* expression is detected in the midgut, are included as a positive control for the *βv* antisense probe. **(B)** RNA *in situ* hybridisation for α-integrin genes *multiple edenomatous wings (mew), inflated (if), scab (scb), αPS4 and αPS5.* No α-integrin transcripts can be detected in stage 2 embryos, suggesting little or no maternal deposition. *mew*, *if* and *scb* transcripts are first detected in cellularising embryos (stage 5), with markedly distinct expression patterns. *if* transcripts are restricted to the presumptive mesoderm (ventral stripe), while *mew* and *scb* are expressed in the dorsal ectoderm, with *mew* transcripts localising to a broad dorsal domain and *scb* transcripts detected in a patch of posterior dorsal cells only. **(C)** RNA *in situ* hybridisation of stage 5 (top row, dorsal view) and stage 6 (bottom row, dorsolateral view) embryos hybridised with *scb* (green) and *mew* (red) probes. Merged and single channel images are shown, as labelled. **(D)** RNA *in situ* hybridisation of stage 5 embryos (lateral views) showing *mew* and *sog* expression patterns, as a merged image (*mew* green, *sog* red) or as individual channels, as labelled. Overlap between *mew* and *sog* expression raises the possibility that mew/αPS1 enhances Sog function by promoting Sog secretion or extracellular movement into the dorsal regions where it binds BMP ligands.

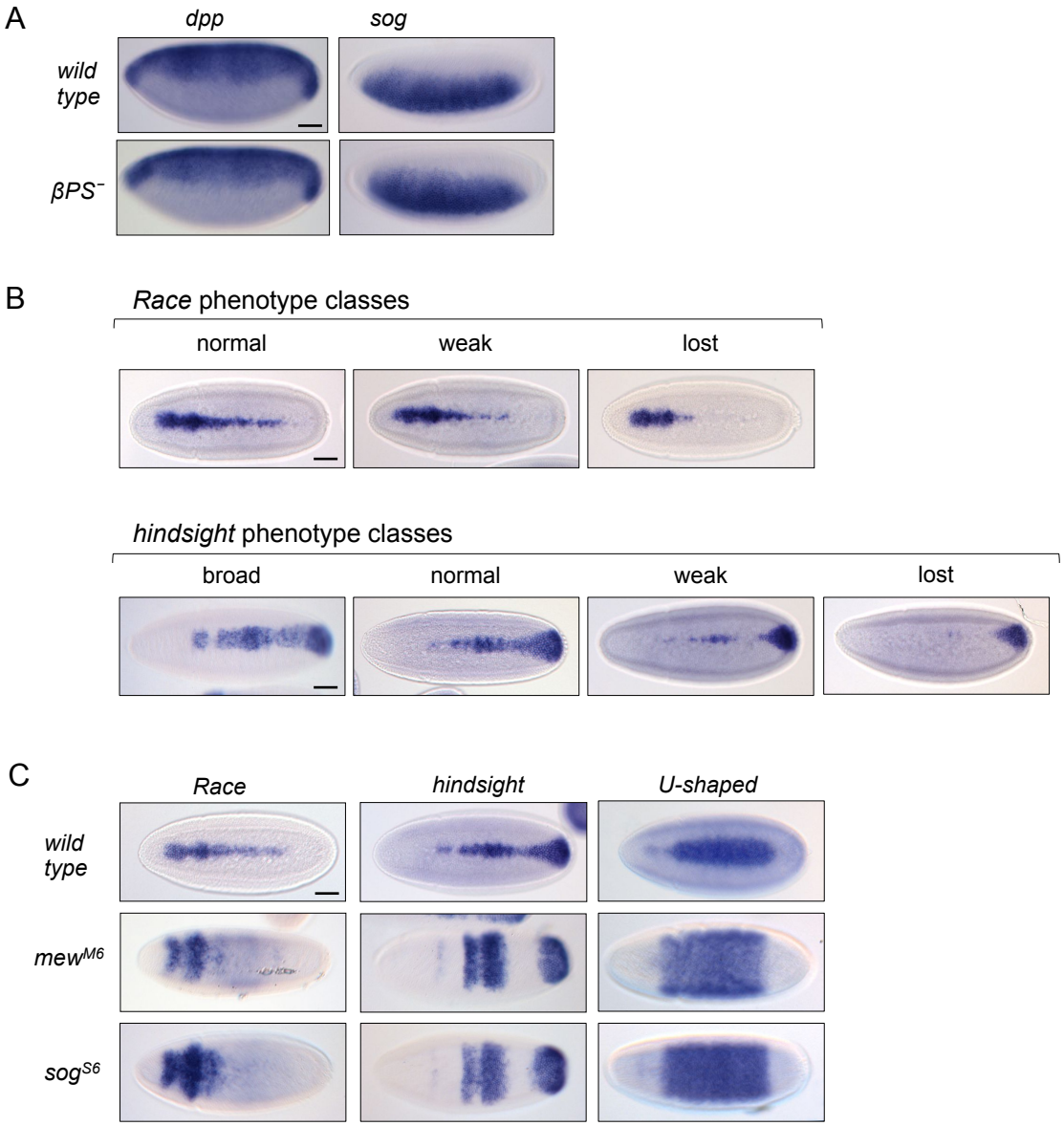

Figure S2, related to Figure 1: Expression patterns of *dpp*, *sog, Race, hnt* and *ush* in embryos lacking βPS. **(A)** RNA *in situ* hybridisations to visualise expression of *dpp* and *sog* in wild-type and *βPS*$^{-}$ embryos. All images show lateral views of stage 5 embryos, anterior to the left. The expression patterns of *sog* and *dpp* are unaffected in *βPS*$^{-}$ embryos. In a sensitised genetic background, integrins in the ovarian follicle epithelium of the mother were previously shown to affect patterning in the embryo by changing the nuclear Dorsal gradient (Negreiros et al., 2010), which sets up the expression patterns of *dpp* and *sog*. The normal expression domains of *dpp* and *sog* expression suggest that the reduction in BMP signaling observed in integrin mutant embryos (see Figure 1) is not due to an earlier defect in the formation of the Dorsal nuclear gradient. This is also consistent with our finding that zygotic expression of βPS is sufficient to rescue the BMP defect in *βPS*$^{-}$ embryos (data not shown). **(B-C)** RNA *in situ* hybridisations for the BMP target genes *Race*, *hindsight (hnt)* and *u-shaped (ush)* in

mew^{M6} and *scb*^{5J38} mutant embryos. **(B)** Expression patterns for *Race* and *hnt* exemplifying the phenotypic classes used for the scoring of phenotypes in *mew* and *scb* mutant embryos, as quantified in Figure 1C. Phenotypes in the rescue experiment of *vkg* mutant embryos in Figure 3 were scored according to the same criteria. **(C)** *sog*$^{-}$-like phenotype observed in *mew*^{M6} integrin mutants. In a small proportion of embryos (~1%), *Race* and *hnt* expression was lost in the central amnioserosa region but expanded laterally in anterior/posterior domains. In ~5% of embryos, expression of *ush* was expanded laterally. These phenotypes are indicative of disrupted BMP gradient formation, with broadened low levels of signaling, resembling the phenotype of *sog*$^{-}$ embryos. Scale bars = 50 μm.

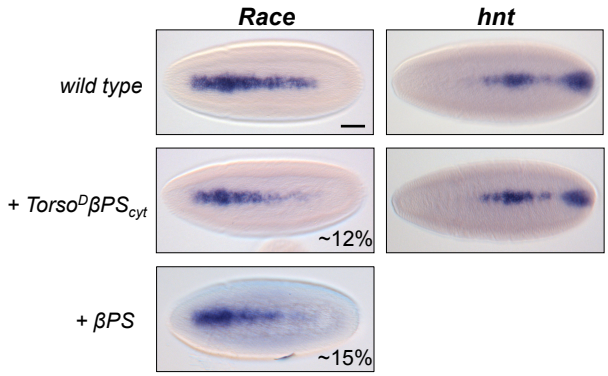

Figure S3, related to Figure 2: Overexpression of Torso^{D}βPS$_{cyt}$ in a wild-type background does not broaden the expression domains of *Race* or *hnt*. RNA *in situ* hybridisations for the BMP target genes *Race* and *hindsight* (*hnt*) in wild-type embryos and embryos overexpressing the Torso^{D}βPS$_{cyt}$ integrin signaling construct or wild-type βPS using the maternal *matαGal4-VP16* driver (see Supplemental Methods for details). *Race* or *hnt* expression is not broadened by ectopic expression of Torso^{D}βPS$_{cyt}$, suggesting that integrin signaling is not sufficient to induce peak threshold BMP target genes outside their normal expression domain. Note that in a small proportion of Torso^{D}βPS$_{cyt}$ overexpressing embryos (~12%) *Race* expression was weakened, an effect also observed in a small proportion of embryos overexpressing wild-type βPS (~15%), as shown. These effects may be due to dominant negative effects of free βPS or Torso^{D}βPS$_{cyt}$ when overexpressed in a wild-type background, as has been reported before (Tanentzapf et al., 2006). All images show dorsal views of stage 6 embryos, anterior to the left. Scale bar = 50 μm.

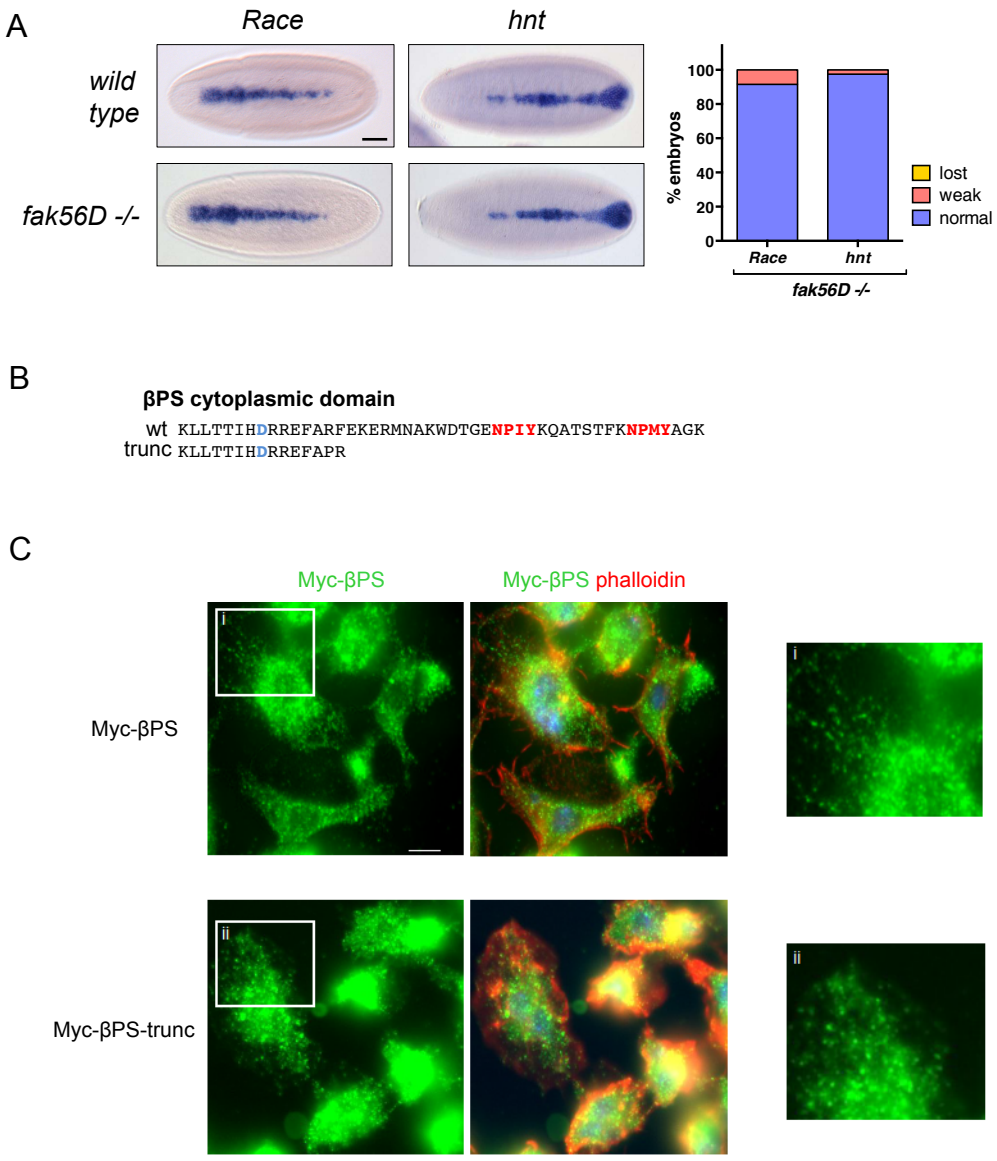

Figure S4, related to Figure 4: Dissecting the mechanism of integrin signaling-mediated enhancement of BMP responses. (A) RNA *in situ* hybridisations for *Race* and *ush* in wild-type and *Fak56D* mutant embryos (dorsal views, stage 6). The *Race* and *hnt* expression patterns are unaffected in the mutant embryos, suggesting that peak BMP expression is FAK-independent. Quantification of phenotypes show counts performed on two repeats. Scale bar = 50μm. **(B)** Amino acid sequence of the cytoplasmic domain of wild-type βPS and the truncation mutant, βPS-trunc, used in the co-immunoprecipitation experiment in Fig. 4J, with the two conserved NPXY motifs highlighted in red, and the salt bridge aspartate (D) residue implicated in the interaction with the α-integrin cytoplasmic domain highlighted in blue. The final two amino acids in βPS-trunc were introduced during the cloning procedure. **(C)** Immunoflourescence images of S2R+ cells expressing Myc-tagged wild-type βPS or the βPS-trunc mutant and plated on collagen IV, and stained with anti-Myc antibody

(green) and phalloidin (red). βPS and βPS-trunc show similar subcellular distribution. Right panels show higher magnification views of regions at the cell periphery outlined in the main figures as as i) (βPS) and ii) (βPS-trunc). Scale bar = 5 μm.

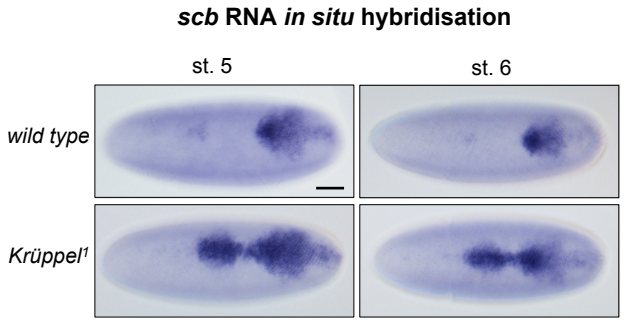

Figure S5, related to Figure 5: *scb* expression in the central domain is repressed by Krüppel.
RNA *in situ* hybridisation for *scb* in wild-type and homozygous *Krüppel*[1] mutant embryos (dorsal views, stage 5 or 6 as indicated). In *Krüppel*[1] mutant embryos, expression of *scb* extends into the central region, consistent with a function for Krüppel in repressing *scb* in this region. Scale bars = 50μm.

Supplemental Experimental Procedures

Fly strains, crosses and phenotype analysis

The following fly strains were used in this study: *mys^{XG43} FRT101* (Leptin et al., 1989), *mew^{M6}* (Bloomington #1483), *scb^{5J38}*, *UAS-mys UAS-srcEGFP*, *UAS-Torso^{D}βPS$_{cyt}$ UAS-mCD8GFP* (Schock and Perrimon, 2003), *UASp-Tkv^{QD}* (Casanueva and Ferguson, 2004), *vkg^{k00236}* (Bloomington #10473), *Fak56D^{CG1}* (Grabbe et al., 2004), *LanB1^{1B1} FRT40A* (Urbano et al., 2009), *matα-Gal4-VP16* (Bloomington BL7062), *dpp^{Hin37}/GlaDp(2;2)DTD48*, *Kr^{1}* (Bloomington #3493). Bloomington strains #1813, #1929 and #2121 were used to generate *mys^{XG43} or LanB1^{1B1}* germ-line clones using the FLP-DFS technique (Chou and Perrimon, 1996). *y^{67c23}w^{118}* flies were used as wild-type controls.

To generate *βPS^{-}* germ-line clones, 3rd instar larvae of the genotype *mys^{XG43} FRT101/ovo^{D1} FRT101; hsFlpase/+* were heat-shocked on two consecutive days for 2h at 37°C. The resulting adult females were crossed as follows to obtain *βPS^{-}* embryos (marked by absence of a *ftz-lacZ* balancer):

♀ *mys^{XG43} FRT101/mys^{XG43} FRT101* x ♂ *FM7c ftz-lacZ/Y* → *mys^{XG43} FRT101/Y*

LanB1^{1B1} germ-line clones were generated similarly by heat-shocking larvae of the genotype *hsFlpase/+; LanB1^{1B1} FRT40A/ovo^{D1} FRT40A*. Resulting adult females were crossed as follows to obtain *LanB1^{1B1}* embryos (marked by absence of *ftz-lacZ* balancer):

♀ *LanB1^{1B1} FRT40A/LanB1^{1B1} FRT40A* x ♂ *LanB1^{1B1} FRT40A/CyO ftz-lacZ*→ *LanB1^{1B1} FRT40/LanB1^{1B1} FRT40A*

For rescue experiments of *βPS^{-}* embryos, *mys^{XG43}* germline clones in females were generated as described above, but with inclusion of a matα4-Gal4-VP16 transgene to allow expression of paternally derived rescue constructs in the embryo. Embryos were collected from the following crosses (presence of UAS-Torso^{D}βPS$_{cyt}$ marked by absence of *ftz-lacZ*):

a) ♀ *mys^{XG43} FRT101 / FRT101 mys^{XG43}; hsFLPase/matα4-Gal4-VP16* X ♂ *yw*

b) ♀ *mys^{XG43} FRT101 / FRT101 mys^{XG43}; hsFLPase/matα4-Gal4-VP16* X ♂ *UAS-mys*

c) ♀ *mys^{XG43} FRT101 / FRT101 mys^{XG43}; hsFLPase/matα4-Gal4-VP16* X ♂ *UAS-Torso^{D}βPS$_{cyt}$/TM3, ftz-lacZ*

For *vkg* rescue experiments, embryos were collected from the following crosses (presence of UAS-Torso^{D}βPS$_{cyt}$ marked by absence of *ftz-lacZ*)::

a) ♀ *vkg^{k00236}/matα4-Gal4-VP16* X ♂ *yw*

b) ♀ *vkg^{k00236}/matα4-Gal4-VP16* X ♂ *UAS-mys*

c) ♀ *vkg*^{k00236}*/matα4-Gal4-VP16* X ♂ *UAS-Torso*^{D}*βPS*$_{cyt}$*/TM3, ftz-lacZ*

To overexpress βPS or Torso^{D}βPS$_{cyt}$ in a wild-type background, embryos were collected from the crosses (presence of UAS-Torso^{D}βPS$_{cyt}$ marked by absence of *ftz-lacZ*):

♀ *matα4-Gal4-VP16 x* ♂ *UAS-Torso*^{D}*βPS*$_{cyt}$*/TM3, ftz-lacZ*

♀ *matα4-Gal4-VP16 x* ♂ *UAS-mys/UAS-mys*

Embryos overexpressing Tkv^{QD} were obtained by collection from mothers with the genotype *matα4-Gal4VP16/+, UASp-Tkv*^{QD}*/+*, allowing Tkv^{QD} expression in the germline and developing oocyte/embryo.

For all other embryo collections, embryos were collected from heterozygous (*vkg*^{k00236}, *mew*^{M6}, *scb*^{5J38}, *dpp*^{Hin37}*/GlaDp(2;2)DTD48*) or homozygous (*Fak56D*^{CG1}) stocks, which were sometimes derived from available stocks by introducing a *ftz-lacZ*-marked balancer.

For the quantification of phenotypes, expression patterns for *Race* and *hindsight* in the central presumptive amnioserosa region were scored as either normal or disrupted, with a disrupted pattern defined as the clear loss of a continuous expression stripe along the dorsal midline. For *mew* and *scb* mutants and the rescue experiments with *vkg* mutant embryos, *Race* and *hindsight* expression was scored in additional categories as weak or broadened (see Figure S2B for examples of each category). For all rescue experiments, the % rescue was calculated as the percentage reduction in the proportion of embryos with a disrupted expression pattern (weak + lost) in the progeny of the rescue cross relative to the proportion seen in the non-transgene control (i.e. crosses to yw, crosses a) above), according to this formula: $\%\ rescue\ for\ (b) = \frac{\%\ disrupted\ in\ (a) - \%\ disrupted\ in\ (b)}{\%\ disrupted\ in\ (a)} \times 100.$

To measure the width of *ush* and *Race* expression (Figures 1B, 3C and 3D), the width of the expression stripe at ~0.5 embryo length in pixels was measured manually for each embryo using Image J. Pixel measurements were then converted into measurements of cell numbers by determining the average cell width in pixels through repeated pixel measurements of a defined number of cell rows along the dorsal midline.

pMad imaging and quantification

Embryos were imaged using a Leica TCS SP5 AOBS inverted confocal microscope using a 20x objective and 1.7x confocal zoom. Images for direct comparison were imaged on the same day with identical settings. Embryos were imaged in 18 consecutive coronal optical sections covering the total depth of the pMad stain, followed by maximal intensity projections of 3D stacks. Quantification was

performed as previously described (Umulis et al., 2010). The analysis comprised three image sets, (images obtained from three independent stainings). Each image set contained four groups: (1) maternal *βPS*$^{-}$, zygotic *βPS*$^{+}$ stage 5; (2) maternal *βPS*$^{-}$, zygotic *βPS*$^{+}$ stage 6, (3) m/z *βPS*$^{-}$ stage 5, (4) m/z *βPS*$^{-}$ stage 6. Stage 6 was marked by appearance of the cephalic furrow. Each group from each set contained at least 6 embryos. One image set was chosen as a reference and intensity values of other sets were scaled (normalised) to this set to allow combination of the data. To calculate the width of the pMad stripe above a certain intensity threshold (Figure 1F, G), the width for each individual embryo was first determined in pixels from each image thresholded at the given intensity. The typical cell diameter in pixels was determined and used to convert the pixel width measurement into a measurement in unit of cells.

DNA constructs and dsRNA preparation

The following expression plasmids have been previously described: pAC-Flag-Mad, pAC-Flag-Tkv^{QD} (Muller et al., 2003). pMT-frizzled-V5 was a gift from Jean-Paul Vincent. To generate pAC-Tkv^{QD}-V5, the coding sequence of Tkv^{QD} from pAC-Flag-Tkv^{QD} was cloned into the XbaI site of pAC5.1A in frame with the C-terminal V5-His tag. For pMT-Myc-Torso^{D}βPS$_{cyt}$, the Myc-Torso^{D}βPS$_{cyt}$ CDS was PCR-amplified from genomic DNA of *UAS-Torso^{D}βPS$_{cyt}$* flies and inserted into pMT (Invitrogen). The βPS (*Drosophila* Genomics Resourse Center) and *α*PS3 (a gift from Nick Brown) cDNAs were inserted into a pMT-Myc vector using In-Fusion HD cloning kit (Clontech) to allow expression of N-terminally tagged integrin subunits. βPS and Torso^{D}βPS$_{cyt}$ cytoplasmic domain mutations (Y831A, Y843A and the double mutant) were generated from pMT-Myc-Torso^{D}βPS$_{cyt}$ by site-directed mutagenesis. The βPS cytoplasmic tail truncation (comprising the last 34 residues) was generated by PCR around the pMT-Myc-βPS using the below primers followed by restriction digestion (Avr2) and ligation.

FW - GCCCTAGGTAGGGCGCGCCTAGATTCGCAATCA

REV - GCCCTAGGAGCGAACTCCCGCCGATCGTGGATC

dsRNA was generated from PCR fragments amplified with the following primers using the Megascript kit (Invitrogen):

bPS FW-TAATACGACTCACTATAGGGTGGACACAGACGATCCACAT

bPS REV-TAATACGACTCACTATAGGGCAACTGGTTCCTGTTCCGTT

aPS1 FW- TAATACGACTCACTATAGGGTCATCGCCACAGTCTTTCTG

aPS1 REV-TAATACGACTCACTATAGGGTTGGCATCTCTATATCCGGC

aPS3 FW-TAATACGACTCACTATAGGGTGGACACAGACGATCCACAT

aPS3 REV -TAATACGACTCACTATAGGGCAACTGGTTCCTGTTCCGTT

RNA was recovered using ammonium acetate and EtOH, dried, resuspended in 20μl of nuclease free water.

DNA Transfections of S2R+ cells

For pMad signaling assays, $3x10^6$ *Drosophila* S2R+ cells were transfected using effectene (Qiagen) and the following amounts of DNA: 250ng pAC-Flag-Mad, 100-500ng of pAC-Flag-Tkv^{QD} and 500ng of pAC-Flag (EV-Flag), pMT-Myc (EV-Myc), pMT-Myc-βPS, pMT-Myc-βPS-trunc or pMT-Myc-$Torso^{D}βPS_{cyt}$ (wild-type or mutant $βPS_{cyt}$ region). For co-immunoprecipitation experiments, $3x10^6$ cells were transfected with 5μg DNA per plasmid. When plating cells on a collagen IV substrate prior to transfection, tissue culture wells were coated with collagen IV by adding 50μg human placental collagen IV (Advanced Biomatrix), diluted with sterile PBS, for 1h at 37°C. Excess unbound collagen IV was removed by rinsing in PBS and cells were then plated as appropriate. For laminin competition experiments, collagen IV-plated cells were treated with a final concentration of 1 or 2μg/mL of mouse laminin (Corning). Laminin was added in serum-free medium 72h post-transfection and cells were harvested 2h after treatment.

Immunostaining of S2R+ cells

S2R+ cells transfected with pMT-Myc-βPS, pMT-Myc-βPS-trunc and plated on collagen IV-coated coverslips were fixed with 4%PFA, followed by incubation overnight with mouse anti-Myc (1:250, Millipore) and Phalloidin dye (1:500, Life Technologies), washes with PBT (PBS with 0.1% Tween 20) and incubation in anti-mouse secondary antibody (Alexa Fluor® 488 dye, 1:500). Stained cells were mounted with Prolong gold antifade reagent with DAPI (Life technologies). Images were captured with an Olympus BX51 upright microscope using a 63x oil immersion objective and Coolsnap EC camera and processed through MetaVue software (Molecular Devices).

Co-Immunoprecipitation experiments

48h after transfection cells were harvested and lysed in NP-40 buffer. Lysates were pre-cleared by incubation with protein G-coupled Agarose beads (Pierce) for 30 min at 4°C. Cleared lysates were incubated with 3ug of anti-αPS1 antibody (DK.1A4, Developmental Studies Hybridoma Bank) for 2h at

4°C followed by incubation with Protein G-coupled Agarose beads for 30 min at 4°C. Lysates were than washed four times in lysis Buffer. For Myc-tagged proteins, complexes were precipitated using anti-Myc agarose beads (Sigma) for 1.5 h at 4°C. Beads were then washed four times with chilled PBS. Protein complexes were resolved by SDS-PAGE and detected by Western blotting.

Supplemental References

Brown, N.H. (2000). Cell-cell adhesion via the ECM: integrin genetics in fly and worm. Matrix Biol *19*, 191-201.

Casanueva, M.O., and Ferguson, E.L. (2004). Germline stem cell number in the Drosophila ovary is regulated by redundant mechanisms that control Dpp signaling. Development *131*, 1881-1890.

Chou, T.B., and Perrimon, N. (1996). The autosomal FLP-DFS technique for generating germline mosaics in Drosophila melanogaster. Genetics *144*, 1673-1679.

Grabbe, C., Zervas, C.G., Hunter, T., Brown, N.H., and Palmer, R.H. (2004). Focal adhesion kinase is not required for integrin function or viability in Drosophila. Development *131*, 5795-5805.

Leptin, M., Bogaert, T., Lehmann, R., and Wilcox, M. (1989). The function of PS integrins during Drosophila embryogenesis. Cell *56*, 401-408.

Muller, B., Hartmann, B., Pyrowolakis, G., Affolter, M., and Basler, K. (2003). Conversion of an extracellular Dpp/BMP morphogen gradient into an inverse transcriptional gradient. Cell *113*, 221-233.

Negreiros, E., Fontenele, M., Camara, A.R., and Araujo, H. (2010). alpha PS1 beta PS integrin receptors regulate the differential distribution of sog fragments in polarized epithelia. Genesis *48*, 31-43.

Schock, F., and Perrimon, N. (2003). Retraction of the Drosophila germ band requires cell-matrix interaction. Genes Dev *17*, 597-602.

Tanentzapf, G., Martin-Bermudo, M.D., Hicks, M.S., and Brown, N.H. (2006). Multiple factors contribute to integrin-talin interactions in vivo. J Cell Sci *119*, 1632-1644.

Umulis, D.M., Shimmi, O., O'Connor, M.B., and Othmer, H.G. (2010). Organism-scale modeling of early Drosophila patterning via bone morphogenetic proteins. Dev Cell *18*, 260-274.

Urbano, J.M., Torgler, C.N., Molnar, C., Tepass, U., Lopez-Varea, A., Brown, N.H., de Celis, J.F., and Martin-Bermudo, M.D. (2009). Drosophila laminins act as key regulators of basement membrane assembly and morphogenesis. Development *136*, 4165-4176.